Synthesis, Crystal Structure and Electrospray Mass Spectrometric Study of the Rhodium(III) Dioxolene Complex $[Rh\{O\overline{CC(CO_2Et)SC(CO_2Et)C}O\}(\eta^5\text{-}C_5Me_5)(PPh_3)]$†

William Henderson,[a]* **John Fawcett**,[b] **Raymond D. W. Kemmitt**[b] and **David R. Russell**[b]
[a] *Department of Chemistry, University of Waikato, Private Bag 3105, Hamilton, New Zealand*
[b] *Department of Chemistry, University of Leicester, University Road, Leicester LE1 7RH, UK*

Reaction of the complexes $[RhCl_2(\eta^5\text{-}C_5Me_5)L]$ [L = PPh_3, pyridine (py) or $P(OPh)_3$] with the cyclic diketones $\overline{XCH(CO_2Et)C(O)C(O)CH}(CO_2Et)$ (X = O or S) and excess silver(I) oxide yields the cyclic rhodium(III) dioxolene complexes $[Rh\{O\overline{CC(CO_2Et)XC(CO_2Et)C}O\}(\eta^5\text{-}C_5Me_5)L]$. The complexes have been fully characterised by elemental analysis, and IR and NMR spectroscopies. A single-crystal X-ray diffraction study on $[Rh\{O\overline{CC(CO_2Et)SC(CO_2Et)C}O\}(\eta^5\text{-}C_5Me_5)(PPh_3)]$ reveals the expected piano-stool co-ordination about the rhodium centre, which is tipped out of the otherwise almost planar dioxolene system. Electrospray mass spectrometry has been used to probe the co-ordination chemistry, specifically demonstrating that the triphenylphosphine ligand is labile, and can be trapped by such reagents as H_2O_2, S_8, Se and $AgNO_3$. The resulting $Ph_3P{=}E$ (E = O, S or Se) ligands show differing tendencies to co-ordinate to the resulting Rh centre. With MeI, the dioxolene ligand is cleaved, *via* alkylated intermediates, and the species $[RhI(C_5Me_5)(NCMe)]^+$ and $[RhI(C_5Me_5)(PPh_3)]^+$ are detected in the resulting reaction mixture, together with PPh_3Me^+.

A wide number of transition-metal complexes containing catecholate and related ligands have been prepared to date,[1] and such complexes are of wide-ranging interest. Their electrochemical behaviour, and inter-relationship with semiquinone complexes have been the subject of a large number of studies.[1,2] Platinum and palladium catecholate complexes have also been synthesised as potential labels for the preparation of metalloantigens,[3] and certain platinum catecholates have been reported to have anticancer activity.[4] Naturally occurring catecholates are found in enterobactins as powerful iron-sequestering agents, and a number of model complexes have been synthesised to mimic such species.[5] There remains a significant, continued interest in the synthesis of new types of semiquinone and catecholate complexes, and recent emphasis has been placed on the synthesis of bimetallic bridged and polymeric complexes.[6]

We recently described the silver(I) oxide-mediated synthesis of a number of related platinum dioxolene complexes **1**, starting from the cyclic diketones **I**.[7] Such dioxolene complexes can be viewed as being derived from parent cyclopentadiene, furan, and thiophene heteroaromatic systems, and thus the diketones **I** offer a route into a potentially wide range of new metal–dioxolene complexes. We wished to explore these possibilities further, and in this paper we report the synthesis and characterisation of some complexes of rhodium(III). The relatively new technique of electrospray mass spectrometry (ESMS) has also been used to probe the co-ordination chemistry of these new complexes, and these results are discussed in terms of the lability of the ancillary neutral donor ligands, specifically triphenylphosphine.

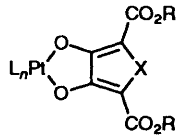

	X	L	R
1a	CH_2	PPh_3	Me
1b	O	PPh_3	Et
1c	O	½cod	Et
1d	S	PPh_3	Et

cod = cycloocta-1,5-diene

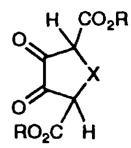

	X	R
Ia	S	Et
Ib	O	Et
Ic	CH_2	Me

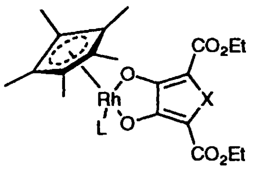

	X	L
2a	S	PPh_3
2b	S	$P(OPh)_3$
2c	O	py
2d	S	$SPPh_3$
2e	S	$SePPh_3$
2f	S	$OPPh_3$

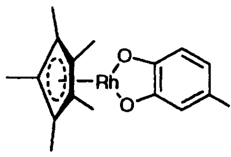

	X
3a	H
3b	Me
3c	Cl

Results and Discussion

Reaction of the rhodium(III) complexes $[RhCl_2(\eta^5\text{-}C_5Me_5)L]$ [L = PPh_3, pyridine (py) or $P(OPh)_3$] with 1 mol equivalent of the cyclic diketone compounds **Ia** or **Ib**, mediated by silver(I) oxide in refluxing dichloromethane gives the rhodium(III)–dioxolene complexes **2a**–**2c** in moderate to good yield as orange to red air-stable crystalline solids. The starting complexes for the synthesis of the pyridine and triphenyl phosphite products were prepared *in situ* by addition of an excess of the ligand to the halide-bridged dimer $[\{RhCl_2(\eta^5\text{-}C_5Me_5)\}_2]$.[8] These dioxolene syntheses may proceed through rhodium-hydroxo complexes, since such species are known to be formed in reactions of the dichloro complex $[RhCl_2(\eta^5\text{-}C_5Me_5)(PMe_3)]$ with Ag_2O.[9]

---

† *Supplementary data available:* see Instructions for Authors, *J. Chem. Soc., Dalton Trans.*, 1995, Issue 1, pp. xxv–xxx.

The triphenylphosphine thiophene-derived dioxolene complex **2a** has been characterised by a single-crystal X-ray diffraction study. The molecular structure is shown in Fig. 1, together with the atom numbering scheme. Table 1 gives details of the X-ray structure determination, while fractional atomic coordinates are given in Table 2, and Tables 3 and 4 present selected intramolecular bond distances and angles, respectively. To the best of our knowledge, there have been only three previous structural determinations on rhodium catecholate-type complexes,[10,11] with only compound **3**[10] being a mononuclear complex, though a number of related semiquinone(1 −) and tropolonate-type complexes have also been structurally characterised.[12]

The structure of **2a** comprises a central rhodium atom, co-ordinated by a pentamethylcyclopentadienyl ligand, a chelating dioxolene ligand and a triphenylphosphine, completing a pseudo-octahedral co-ordination arrangement in the expected piano-stool type geometry. The overall structural features are largely as would be expected for a complex of this type. In particular, the organic dioxolene moiety displays a strong resemblance, with similar bond lengths and angles, to the cyclopentadiene-derived platinum(II) complex **1a** reported by us previously.[7] The dioxolene ligand itself shows little deviation from planarity, with no atom more than 0.08 Å from the least-squares plane passing through the dioxolene ligand atoms. The rhodium atom is shifted by 0.358 Å out of the least-squares dioxolene plane, towards the cyclopentadienyl ligand. The slight twist-fold of the rhodium-dioxolene group is confirmed by the angle of 13.46(12)° between the O(1)–Rh–O(2) plane and the least-squares plane of the dioxolene ligand. The substituent carbonyl groups are also largely coplanar with the dioxolene ligand, as evidenced by the torsion angles O(3)–C(15)–C(13)–S [9.38(61)] and O(5)–C(18)–C(14)–S [3.07(51)°], though the substituent ethyl esters are slightly displaced out of the Rh–dioxolene plane, in a *trans*-arrangement. The bond distances within the dioxolene ligand are comparable with those in the related platinum complex **1a**,[7] and are largely consistent with C–O–Rh single bonds, and C(11)–C(13) and C(12)–C(14) bonds containing a substantial amount of double bond character. The Rh–P distance appears similar to other Rh–P bond distances in η^5-C_5Me_5 rhodium(III) complexes, *e.g.* 2.335(1) Å in **2a** compared to 2.319(5) Å in [Rh(η^5-C_5Me_5)(O_2CMe)$_2$(PMe_3)][9] and 2.383(1) Å in [Rh(η^5-C_5Me_5)(NO_3)$_2$(PPh_3)].[13]

The bonding of the pentamethylcyclopentadienyl ligand to the rhodium atom appears to be somewhat irregular, with rhodium-carbon bond distances in the range 2.154(4)–2.204(4) Å, with a mean of 2.177 Å, which is comparable with that in [Rh(η^5-C_5Me_5)(O_2CMe)$_2$(PMe_3)], 2.16(2) Å.

In addition to molecules of **2a**, the structure contains one solvent molecule of water per rhodium complex in the lattice. It would appear that this water molecule is relatively easily removed, since on vacuum drying crystals for elemental microanalysis they were observed to lose solvent. Analytical data support the non-solvated complex rather than the monohydrate. The closest non-bonded contacts of oxygen O(7) of the water molecule are to the dioxolene oxygen O(2) (2.889 Å) and the ester oxygen O(6) (3.018 Å).

The NMR spectroscopic features of the dioxolene complexes **2a**–**2c** are in accord with their structures. The C_5Me_5 protons of the triphenyl-phosphine and -phosphite complexes **2a** and **2b** show coupling to ^{31}P of 3.0 and 5.1 Hz respectively in their ^1H NMR spectra. The rhodium catecholate complexes **4**, containing PPh_3 ligands, were previously reported not to show any ^{31}P coupling to the C_5Me_5 hydrogens, and this was taken as evidence that these complexes are labile in solution.[10] The strength of binding of the phosphine was found to be related to the presence of electronegative substituents on the catecholate ligand, and since in the complex **2a** there are two electron-withdrawing CO_2Et groups, this would be expected to stabilise the PPh_3 complex. From electrospray mass spectrometry however, we have obtained evidence that the PPh_3 ligand in **2a** retains significant lability, as discussed later.

Table 1 Crystal data for [Rh{OCC(CO_2Et)SC(CO_2Et)CO}(C_5Me_5)(PPh_3)]·H_2O **2a·H_2O**

Empirical formula	$C_{38}H_{40}O_6PRhS{\cdot}H_2O$
M	776.69
Crystal system	Monoclinic
Space group	$P2_1/n$
a/Å	13.630(2)
b/Å	17.381(2)
c/Å	15.250(2)
β/°	92.19(1)
U/Å^3	3610.1(8)
D_c/g cm^{-3}	1.278
Z	4
F(000)	1440
Absorption coefficient/mm^{-1}	0.605

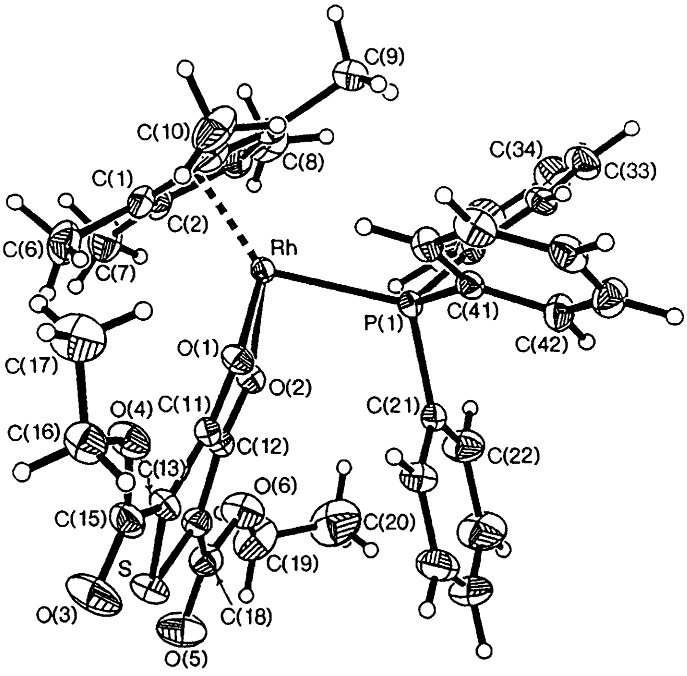

Fig. 1 Molecular structure of the complex [Rh{OCC(CO_2Et)SC(CO_2Et)CO}(C_5Me_5)(PPh_3)]·H_2O **2a·H_2O**, showing the atom numbering scheme. Atoms are shown as thermal ellipsoids at the 30% probability level, with the exception of the H atoms which are depicted as arbitrary spheres in their calculated positions. The water molecule of crystallisation is not shown

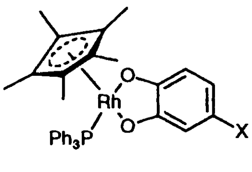

4 X = H, Me, Cl

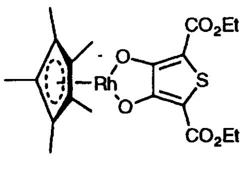

5

The ^{13}C-{^1H} and ^1H NMR spectra of the dioxolene–rhodium fragment are overall very similar to those of the related platinum(II) complexes **1** reported previously,[7] excepting the ^{13}C couplings to the metals ^{103}Rh ($I = \frac{1}{2}$, 100% abundant) and ^{195}Pt ($I = \frac{1}{2}$, 33% abundant), the former couplings being substantially smaller and typically not resolvable. Accordingly, resonances were assigned by direct comparison of their chemical shifts with the platinum complexes.

Table 2 Fractional atomic coordinates (× 10⁴) for $[Rh\{O\overline{CC(CO_2Et)SC(CO_2Et)C}O\}(C_5Me_5)(PPh_3)]\cdot H_2O$ **2a**·H_2O

Atom	*x*	*y*	*z*	Atom	*x*	*y*	*z*
Rh	2 359(1)	7 547(1)	8 992(1)	C(16)	−1 042(3)	9 773(2)	9 252(3)
P	3 377(1)	7 790(1)	10 227(1)	C(17)	−528(4)	10 132(3)	8 502(4)
S	−842(1)	7 122(1)	10 693(1)	C(18)	193(3)	5 790(2)	10 908(3)
O(1)	1 248(2)	8 195(1)	9 539(2)	C(19)	1 148(5)	4 648(3)	11 149(4)
O(2)	1 723(2)	6 685(1)	9 762(2)	C(20)	2 103(5)	4 602(4)	11 610(4)
O(3)	−1 695(2)	8 686(2)	10 338(3)	C(21)	2 862(2)	7 502(2)	11 268(2)
O(4)	−497(2)	9 075(2)	9 472(2)	C(22)	3 177(3)	6 871(3)	11 745(3)
O(5)	−486(3)	5 525(2)	11 297(2)	C(23)	2 771(4)	6 723(4)	12 549(4)
O(6)	1 024(2)	5 417(2)	10 787(2)	C(24)	2 062(4)	7 181(4)	12 865(3)
C(1)	1 685(3)	7 685(2)	7 682(2)	C(25)	1 732(4)	7 791(3)	12 379(3)
C(2)	2 086(3)	6 949(2)	7 732(2)	C(26)	2 126(3)	7 951(3)	11 590(3)
C(3)	3 124(3)	7 015(2)	7 924(2)	C(31)	4 574(3)	7 324(2)	10 204(2)
C(4)	3 359(3)	7 815(2)	7 959(2)	C(32)	5 451(3)	7 727(2)	10 291(2)
C(5)	2 471(3)	8 229(2)	7 821(2)	C(33)	6 345(3)	7 349(3)	10 265(3)
C(6)	632(3)	7 900(3)	7 539(3)	C(34)	6 368(3)	6 571(3)	10 169(3)
C(7)	1 548(4)	6 198(3)	7 620(3)	C(35)	5 510(4)	6 157(3)	10 071(3)
C(8)	3 840(4)	6 361(3)	7 916(3)	C(36)	4 612(3)	6 531(2)	10 079(3)
C(9)	4 369(3)	8 151(3)	8 063(3)	C(41)	3 638(2)	8 801(2)	10 446(2)
C(10)	2 350(4)	9 078(3)	7 708(3)	C(42)	4 146(3)	9 032(2)	11 214(3)
C(11)	614(2)	7 732(2)	9 888(2)	C(43)	4 334(3)	9 803(2)	11 370(3)
C(12)	886(2)	6 939(2)	10 064(2)	C(44)	4 008(3)	10 346(2)	10 770(3)
C(13)	−317(3)	7 895(2)	10 154(3)	C(45)	3 491(3)	10 130(2)	10 030(3)
C(14)	191(3)	6 552(2)	10 525(2)	C(46)	3 304(3)	9 356(2)	9 865(3)
C(15)	−912(3)	8 576(2)	10 018(3)	O(7)	−2 492(3)	4 821(2)	10 621(2)

Table 3 Selected intramolecular bond lengths (Å) for $[Rh\{O\overline{CC(CO_2Et)SC(CO_2Et)C}O\}(C_5Me_5)(PPh_3)]\cdot H_2O$ **2a**·H_2O

Rh–O(1)	2.086(2)	Rh–O(2)	2.111(2)
Rh–C(1)	2.180(4)	Rh–C(2)	2.204(4)
Rh–C(3)	2.172(4)	Rh–C(4)	2.173(4)
Rh–C(5)	2.154(4)	Rh–P	2.3352(9)
P–C(21)	1.830(3)	P–C(31)	1.823(3)
P–C(41)	1.821(4)	S–C(13)	1.743(4)
S–C(14)	1.748(4)	O(1)–C(11)	1.309(4)
O(2)–C(12)	1.321(4)	O(3)–C(15)	1.205(4)
O(4)–C(15)	1.342(5)	O(4)–C(16)	1.454(5)
O(5)–C(18)	1.211(5)	O(6)–C(18)	1.324(5)
O(6)–C(19)	1.453(5)	C(1)–C(2)	1.392(6)
C(1)–C(5)	1.438(6)	C(1)–C(6)	1.492(6)
C(2)–C(3)	1.438(5)	C(2)–C(7)	1.503(6)
C(3)–C(4)	1.428(6)	C(3)–C(8)	1.499(6)
C(4)–C(5)	1.417(6)	C(4)–C(9)	1.498(5)
C(5)–C(10)	1.493(6)	C(11)–C(13)	1.376(5)
C(11)–C(12)	1.449(5)	C(12)–C(14)	1.377(5)
C(13)–C(15)	1.446(5)	C(14)–C(18)	1.447(5)
C(16)–C(17)	1.500(6)	C(19)–C(20)	1.457(8)
Triphenylphosphine ligand			
C–C 1.355(7)–1.396(5), mean 1.378(6)			

Table 4 Selected intramolecular bond angles (°) for $[Rh\{O\overline{CC(CO_2Et)SC(CO_2Et)C}O\}(C_5Me_5)(PPh_3)]\cdot H_2O$ **2a**·H_2O

O(1)–Rh–O(2)	80.86(9)	O(1)–Rh–P	89.85(7)
O(2)–Rh–P	85.63(7)	C(31)–P–C(41)	105.3(2)
C(31)–P–C(21)	105.5(2)	C(41)–P–C(21)	100.5(2)
C(21)–P–Rh	114.46(11)	C(31)–P–Rh	114.16(12)
C(41)–P–Rh	115.42(12)		
Dioxolene ligand			
C(11)–O(1)–Rh	109.3(2)	C(12)–O(2)–Rh	109.5(2)
C(13)–S–C(14)	91.1(2)	C(15)–O(4)–C(16)	117.3(3)
C(18)–O(6)–C(19)	119.1(4)	O(1)–C(11)–C(13)	128.6(3)
O(1)–C(11)–C(12)	119.4(3)	C(13)–C(11)–C(12)	111.9(3)
O(2)–C(12)–C(14)	129.3(3)	O(2)–C(12)–C(11)	118.2(3)
C(14)–C(12)–C(11)	112.5(3)	C(11)–C(13)–C(15)	130.1(4)
C(11)–C(13)–S	112.4(3)	C(15)–C(13)–S	117.4(3)
C(12)–C(14)–C(18)	131.5(4)	C(12)–C(14)–S	111.8(3)
C(18)–C(14)–S	116.6(3)	O(3)–C(15)–O(4)	123.3(4)
O(3)–C(15)–C(13)	124.9(4)	O(4)–C(15)–C(13)	111.8(3)
O(4)–C(16)–C(17)	105.9(3)	O(5)–C(18)–O(6)	123.8(4)
O(5)–C(18)–C(14)	123.8(4)	O(6)–C(18)–C(14)	112.4(3)
O(6)–C(19)–C(20)	108.9(5)		
C_5Me_5 ligand			
C(1)–C(2)–C(3)	108.6(4)	C(2)–C(1)–C(5)	108.0(4)
C(4)–C(3)–C(2)	107.6(4)	C(5)–C(4)–C(3)	107.4(4)
C(4)–C(5)–C(1)	108.3(4)	C(6)–C(1)–Rh	122.0(3)
C(7)–C(2)–Rh	125.0(3)	C(8)–C(3)–Rh	131.4(3)
C(9)–C(4)–Rh	127.3(3)	C(10)–C(5)–Rh	128.9(3)
C–C–Me	123.7(4)–127.7(4), mean 125.8(4)		
C–C–Rh	69.6(2)–72.4(2), mean 70.9(2)		
Triphenylphosphine ligand			
C–C–C	118.7(4)–121.3(5), mean 120.0(4)		
C–C–P	117.6(3)–123.7(3), mean 120.7(3)		

Electrospray Mass Spectrometry (ESMS) Study of Rhodium–Dioxolene Complexes.—Electrospray mass spectrometry[14] is a versatile and increasingly important technique for the characterisation of co-ordination and organometallic complexes, but to date has still only been applied to a relatively small number of systems.[15] The advantages of the technique are that it can be applied to high molecular weight, as well as ionic species; since it uses a very soft ionisation technique, existing ions in solution are transferred to the gaseous state relatively intact. We have used this technique to probe the co-ordination chemistry of the rhodium(III)–dioxolene complexes, in particular with regard to the lability of the phosphine (or other neutral donor) ligand in the complexes **2a**–**2c**. The relative lack of lability of the ligands in **2a**–**2c** can be in part deduced from the observation of couplings to ^{103}Rh in the NMR spectra.[10] ESMS offered an alternative rapid means of investigating the co-ordination properties with very small quantities of material.

The use of the ESMS technique for the analysis of individual compounds involving rapid ligand exchange has been described previously,[16] and can be considered as an alternative technique to low-temperature NMR studies. As far as we are aware, this is the first example of the application of the technique to dioxolene or related catecholate complexes.

Table 5 Selected electrospray mass spectrometry data for rhodium dioxolene complexes[a]

Complex	Ions (m/z)[b]
2a	$[2M + H]^+$ (1518), $[M + H]^+$ (759), $[M - PPh_3 + H]^+$ (497)
2b	$[2M + H]^+$ (1613), $[2M - P(OPh)_3 + H]^+$ (1303), $[2M - 2P(OPh)_3 + H]^+$ (993), $[M + H]^+$ (807), $[M - P(OPh)_3 + NH_4]^+$ (514), $[M - P(OPh)_3 + H]^+$ (497)
2c	$[M + H]^+$ (560), $[M - py + NH_4]^+$ (498), $[M - py + H]^+$ (481), plus a number of unassigned peaks in the region m/z 100–400
2a + S_8	$[2M - PPh_3 + S + H]^+$ (1287), $[2M - PPh_3 + H]^+$ (1255), $[M + S + H]^+$ (791), $[M + H]^+$ (759), $[M - PPh_3 + S + H]^+$ (529), $[M - PPh_3 + H]^+$ (497), $[Ph_3PS + H]^+$ (295)
2a + Se	$[2M - PPh_3 + Se + H]^+$ (1335), $[2M - PPh_3 + H]^+$ (1255), $[2M - 2PPh_3 + H]^+$ (993), $[M + Se + H]^+$ (839), $[M + H]^+$ (759), $[M - PPh_3 + H]^+$ (497)
2a + H_2O_2	$[2M - PPh_3 + H]^+$ (1255), $[M + O + H]^+$ (775), $[M + H]^+$ (759), $[M - PPh_3 + H]^+$ (497), $[Ph_3PO + H]^+$ (279)
2a + $AgNO_3$	$[M + Ag]^+$ (865, 867), $[M + H]^+$ (759), $[M - PPh_3 + Ag^+ + MeCN]^+$ (644, 646), $[M - PPh_3 + H]^+$ (497), $[(Ph_3P)Ag(NCMe)]^+$ (410, 412), $[(Ph_3P)Ag]^+$ (369, 371), $[Ag(NCMe)_2]^+$ (189, 191), $[Ag(NCMe)]^+$ (148, 150)
2a + MeI	New species observed due to $[M + Me]^+$ (773), $[M - PPh_3 + Me]^+$ (511), and on further standing, $[RhI(C_5Me_5)(NCMe)]^+$ (406) and $[RhI(C_5Me_5)(PPh_3)]^+$ (627).

[a] Data are presented as composites over the range of cone voltages employed, to show the total range of species observed. Peaks are identified by the most intense peak (or peaks in the case of silver complexes) in the isotope pattern. [b] M refers to the parent species, *viz.* **2a**–**2c**.

Rhodium–dioxolene complexes. All complexes **2a**–**2c** yield good ESMS spectra using an acetonitrile–water (1:1) mobile phase. A summary of the data is presented in Table 5, and is illustrated by the rhodium triphenylphosphine dioxolene complex **2a** as a typical example for discussion. At a low cone voltage of 25 V, complex **2a** gives a strong parent ion $[M + H]^+$ at m/z 759, and there is excellent agreement between the observed and calculated isotope patterns. In addition to the parent ion peak, there is a peak due to the dimer $[2M + H]^+$ at m/z 1518, plus a small peak at m/z 497 which is assigned to the species $[M - PPh_3 + H]^+$, *i.e.* protonated **5**. Five-co-ordinate species of this type have been structurally characterised previously, *viz.* complex **3a**, by Maitlis and co-workers.[10] Small peaks in the spectrum at m/z 263 and 279 can be ascribed to Ph_3PH^+ and $Ph_3P(O)H^+$ respectively, from the labilised triphenylphosphine ligand. Upon increasing the cone voltage to 45 V, the peaks at m/z 497 and 759 are of approximately equal intensity and at 65 V, the major peak becomes **5** at m/z 497. An additional small peak, as yet unassigned, is also observed at m/z 451. Fig. 2 illustrates the effect of two different cone voltages on the spectrum of **2a**, which effects the increased loss of PPh_3 from the complex.

Overall the ESMS behaviour of the triphenyl phosphite and pyridine complexes **2b** and **2c** appears similar to that of the PPh_3 complex, with both species giving predominant $[M + H]^+$ ions (see Table 5). For both complexes the appropriate species formed by loss of the phosphite or pyridine was observed, at m/z 497 or 481 respectively; that for the pyridine complex was quite an intense peak at a low cone voltage (25 V) suggesting relatively weak metal–ligand bonding. For **2b**, higher clusters such as $[2M - 2P(OPh)_3 + H]^+$ (m/z 993) and $[2M - P(OPh)_3 + H]^+$ (m/z 1303) appeared to be quite prominent, possibly as a result of the additional oxygen atoms of the ligands, which will increase aggregation *via* hydrogen-bonded interactions.

With added sulfur or selenium. An alternative means of investigating ligand lability (in addition to cone voltage variation) is to add a reagent which reacts with and thus traps the ligand if it dissociates from the metal centre. For the PPh_3 complex **2a** this is readily accomplished by addition of either elemental sulfur or selenium, or hydrogen peroxide. Addition of excess S_8 to the aqueous acetonitrile solution of complex **2a** resulted in a rapid lightening of the pale orange solution. The ESMS spectrum, at a cone voltage of 20 V, showed a major peak at m/z 791, tentatively ascribed to the triphenylphosphine sulfide complex **2d**. A number of minor peaks were observed including those due to $[\mathbf{5} + H]^+$ (m/z 497) and $[\mathbf{2a} + H]^+$ (m/z 759), together with a very minor peak due to the species $[M - PPh_3 + S + H]^+$ (m/z 529). Minor peaks at m/z 1255 and 1287 are also assigned to $[2M - PPh_3 + H]^+$, and the phosphine sulfide species $[2M - PPh_3 + S + H]^+$ respectively, where M = **2a**. At a cone voltage of 50 V, the major species in the ESMS spectrum was due to $[\mathbf{5} + H]^+$, formed by loss of the phosphine sulfide ligand. A minor peak at m/z 295 due to $[Ph_3PS + H]^+$ was also observed, but this was small, even at higher cone voltages, presumably as a result of the relatively low basicity of the ligand.

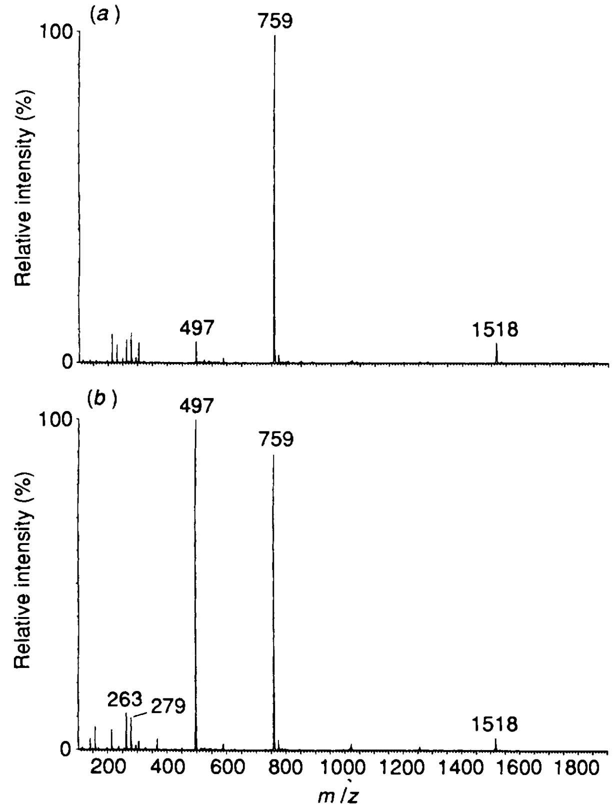

Fig. 2 Electrospray mass spectra of complex **2a**, recorded at cone voltages of (*a*) 25 and (*b*) 45 V, to show the effect on the loss of PPh_3 from the complex

Similar behaviour was observed on addition of elemental (grey) selenium to an aqueous acetonitrile solution of **2a** and immediately recording the ESMS spectrum. Observed peaks and their proposed assignments are listed in Table 5. In this case, the distinctive isotope pattern provided by the six selenium isotopes gives additional supporting evidence for the assignment of the species at *m*/*z* 839 to the phosphine selenide complex **2e**. In this case, the formation of higher aggregates appeared more prevalent than in the sulfur case, and peaks at *m*/*z* 993, 1255 and 1335 are assigned to $[\mathbf{25} + H]^+$, $[2M - PPh_3 + H]^+$, and the phosphine selenide complex $[2M - PPh_3 + Se + H]^+$ respectively (M = **2a**).

These ESMS results are consistent with the presence of an equilibrium in solution involving labilisation of the PPh_3 ligand. Once the phosphine is in solution it reacts forming Ph_3PS, which is also a moderately good ligand towards the rhodium centre. However, results obtained from following the reaction with sulfur by $^{31}P-\{^1H\}$ NMR support the results from ESMS only in part. Addition of an excess of S_8 to a solution of **2a** in $CDCl_3$ results in a diminution of the peaks due to **2a**, with concomitant increase of a resonance at δ 43.3, subsequently identified as triphenylphosphine sulfide by comparison with the spectrum of an authentic sample. No coupling to ^{103}Rh was observed. Coincidence of the resonances due to free and co-ordinated Ph_3PS, together with a small and unresolved $^2J(^{31}P-^{103}Rh)$ coupling, is an unlikely possibility, but which cannot be discounted. Alternatively, it is possible that in the ESMS experiment, the means by which the ions are formed is causing recombination of the triphenylphosphine sulfide or selenide with the rhodium complex **5**, giving the observed adducts **2d** and **2e**. These observations may suggest that care is required when interpreting ESMS results in the absence of other spectroscopic data. Nevertheless, ESMS still provides a rapid means of screening the reactivity of a species towards other reagents.

With added hydrogen peroxide. As with sulfur and selenium, hydrogen peroxide reacts rapidly with tertiary phosphines, forming phosphine oxides, R_3PO. Unlike phosphine sulfides and selenides however, 'hard' phosphine oxides are typically poor ligands towards the soft platinum group metals, and are better known for their excellent ligand properties towards oxophilic transition, lanthanide and actinide metals. Addition of a small quantity of H_2O_2 to an aqueous acetonitrile solution of **2a** and recording the ESMS spectrum (cone voltage 20 V) after *ca.* 10 min yielded major peaks assigned as $[\mathbf{5} + H]^+$ (*m*/*z* 497), and $[Ph_3PO + H]^+$ (*m*/*z* 279). In addition, smaller peaks assigned as $[\mathbf{2a} + H]^+$ (*m*/*z* 759), the triphenylphosphine oxide complex $[M + O + H]^+$ ($[\mathbf{2f} + H]^+$) (*m*/*z* 775), and $[2M - PPh_3 + H]^+$ (M = **2a**) (*m*/*z* 1255) were also observed, together with a number of other minor species, as yet unidentified. That the peak due to the phosphine oxide complex **2f** is smaller than the peak due to **5** is consistent with the relatively poor donor properties of the ligand towards rhodium, when compared to the analogous phosphine sulfide and selenide.

With added $AgNO_3$. Addition of a few drops of dilute $AgNO_3$ solution to the solution of **2a** and immediately recording the spectrum (cone voltage 25 V) results in an increase of the peak at *m*/*z* 497 due to **5**, and a decrease in the $[M + H]^+$ peak at *m*/*z* 759. Additional peaks were observed in the spectrum due to triphenylphosphine–silver species; $[(Ph_3P)Ag(NCMe)]^+$ (*m*/*z* 410, 412) and $[(Ph_3P)Ag]^+$ (369, 371), together with the expected Ag–MeCN species as indicated in Table 5. Species containing Ag are readily identified by their characteristic isotope pattern due to the presence of approximately equally abundant ^{107}Ag and ^{109}Ag isotopes. A small double peak at *m*/*z* 865, 867 is assigned to the molecular ion $[M + Ag]^+$. After standing for *ca.* 10 min and re-recording the spectrum, the parent ion at *m*/*z* 759 had almost disappeared, and the major peak in the spectrum (in the range *m*/*z* 250–1500) was due to $[(Ph_3P)Ag(NCMe)]^+$ at *m*/*z* 410, 412, whilst peaks due to other PPh_3–Ag species were identifiable as indicated in Table 5, together with a number of minor, unidentified species. Presumably the Ag^+ ion complexes the dissociated PPh_3 more strongly, preventing recombination with the rhodium.

With added iodomethane. Alkylating agents such as iodomethane are another class of reagent capable of reacting with tertiary phosphine ligands, forming quaternary phosphonium salts. We wished to investigate these systems, since unlike the above systems, phosphonium salt formation is completely irreversible, and the positively charged phosphonium salts have no co-ordinating ability whatsoever. Addition of excess MeI to an aqueous acetonitrile solution of **2a**, followed by recording the ESMS spectrum (cone voltage 20 V) after *ca.* 5 min showed substantial amounts of the parent species $[M + H]^+$ and $[2M + H]^+$ at *m*/*z* 759 and 1518 respectively. In addition, a significant peak due to the phosphonium salt PPh_3Me^+ at *m*/*z* 277, together with a small peak at *m*/*z* 773 assigned to $[M + Me]^+$ were observed. On recording the spectrum at a cone voltage of 50 V, additional peaks due to $[\mathbf{5} + H]^+$ and $[\mathbf{5} + Me]^+$ at *m*/*z* 497 and 511 were also observed, in comparable fashion to that described earlier, in the absence of MeI. The nature of the methylated rhodium species can only be speculated upon, based on the available data. The most likely possibilities would include species methylated either at the thiophene sulfur or dioxolene oxygen atoms. Thiophenes are known to be unreactive towards all but the most powerful alkylating agents, such as Me_3O^+ and $MeOSO_2F$.[17] Upon standing for *ca.* 7 h, the reaction mixture is cleanly transformed into two species, together with the PPh_3Me^+ ion. The new species, at *m*/*z* 406 and 627, can be assigned to the complexes $[RhI(C_5Me_5)(NCMe)]^+$ and $[RhI(C_5Me_5)(PPh_3)]^+$ respectively, with both complexes having lost their dioxolene ligands. It appears that alkylation at the oxolene oxygen atoms converts the ligand into a good leaving group, resulting in formation of the observed iodo complexes. Presumably, the observation of PPh_3 ligand in one of the products suggests that alkylation of labilised PPh_3 is in competition with alkylation and loss of the oxolene ligand; PPh_3 ligands in a cationic rhodium complex will be less labile and not subject to the same alkylation reaction as in the parent dioxolene complex **2a**.

It is finally worth noting that the actual iodo complex ultimately formed in solution from the MeI reaction is not clear from ESMS, since halide ligands are readily lost from parent complexes, to generate a cationic species detectable by ESMS. For example, a freshly prepared solution of $[RhCl_2(\eta^5-C_5Me_5)(PPh_3)]$[8] in aqueous acetonitrile yields a major peak due to $[RhCl(\eta^5-C_5Me_5)(PPh_3)]^+$, and no (protonated) parent species is observed. Similar behaviour has been observed for a wide number of other transition-metal halide complexes.[18] Therefore the actual products in solution may be $[RhI_2(\eta^5-C_5Me_5)(NCMe)]$ and $[RhI_2(\eta^5-C_5Me_5)(PPh_3)]$.

ESMS is a versatile method for rapidly investigating reactions of co-ordinated ligands in these rhodium–dioxolene complexes; the application to other co-ordination and organometallic complexes is currently under investigation, and will be reported in due course.

Experimental

All the compounds described in this paper are air- and moisture-stable, and reactions were carried out and products recrystallised from AR grade, but undried solvents, without regard for the exclusion of air. Light petroleum refers to the fraction of b.p. 40–60 °C. The compounds $[\{RhCl_2(\eta^5-C_5Me_5)\}_2]$ and $[RhCl_2(\eta^5-C_5Me_5)(PPh_3)]$ were prepared by the literature procedures.[8] Other chemicals were of reagent grade and were used as supplied. The cyclic diketones **I** were obtained as described previously.[7]

Melting points were recorded on a Reichert hot-stage apparatus and are uncorrected. Infrared spectra were recorded as KBr disks on a Bio-Rad FTS-40 spectrophotometer. Proton NMR spectra were recorded in $CDCl_3$ solution on a Bruker AC300P spectrometer at 300.13 MHz, with chemical shifts referenced to $SiMe_4$ (δ 0.0); $^{13}C-\{^1H\}$ NMR spectra were recorded in $CDCl_3$ on a Bruker AC300P spectrometer at 75.47 MHz relative to $SiMe_4$ (δ 0.0) and $^{31}P-\{^1H\}$ NMR spectra were recorded on a JEOL FX90Q spectrometer at 36.23 MHz respectively, with external 85% H_3PO_4 (δ 0.0) as reference. Electrospray mass spectra were obtained using a VG Platform II mass spectrometer using acetonitrile–water (1:1) as the mobile phase, in positive-ion mode. The compounds were dissolved in the mobile phase to give a solution typically of approximate concentration 0.1 mmol dm^{-3}. The diluted solution was injected into the spectrometer *via* a Rheodyne injector fitted with a 10 μl sample loop. A Thermo Separation Products SpectraSystem P1000 LC pump delivered the solution to the mass spectrometer source at a flow rate of 0.01 ml min^{-1}, and nitrogen was employed both as a drying and nebulising gas. Fragmentation of the parent compounds was investigated by varying the cone voltage between 15 and 65 V.

Syntheses.—$[\mathrm{Rh\{OCC(CO_2Et)SC(CO_2Et)CO\}}(\eta^5\text{-}\mathrm{C_5Me_5})(\mathrm{PPh_3})]\cdot\mathrm{H_2O}$ **2a**·H_2O. A solution of $[\mathrm{RhCl_2}(\eta^5\text{-}\mathrm{C_5Me_5})(\mathrm{PPh_3})]$ (100 mg, 0.187 mmol) and **Ia** (49 mg, 0.188 mmol) in dichloromethane (30 cm^3) was refluxed with excess silver(I) oxide (*ca.* 0.5 g) for 12 h. The resulting red solution was filtered to remove the silver salts, and reduced in volume to *ca.* 5 cm^3. Addition of light petroleum (*ca.* 70 cm^3) gave, on standing, red-orange microcrystals of **2a**·H_2O (109 mg, 77%). Slow recrystallisation from dichloromethane–light petroleum gave dark red crystals of X-ray crystallographic quality. Crystals for elemental microanalysis and NMR spectroscopy were dried under vacuum, whereupon they appeared to lose solvent of crystallisation (Found: C, 59.85; H, 5.55. $C_{38}H_{40}O_6PRhS$ requires C, 60.15; H, 5.30%. $C_{38}H_{40}O_6PRhS\cdot H_2O$ requires C, 58.75; H, 5.45%), m.p. softens > 135 °C, > 180 °C (decomp.); ν(C=O) at 1661 cm^{-1}. NMR: ^{31}P-{^{1}H}, δ 30.3 [d, ^1J(RhP) 159]; ^{1}H, δ 7.68–7.26 (m, 15 H, Ph), 4.14 [q, 4 H, CH_2, ^3J(HH) 7.1], 1.34 [d, 15 H, η^5-C_5Me_5, J(PH) 3.0] and 1.26 [t, 6 H, CH_3 of ethyl, ^3J(HH) 7.1]; ^{13}C-{^{1}H}, δ 173.0 (s, RhOC*C*), 163.6 (s, *C*O$_2$Et), 134.7–128.0 (m, Ph), 99.7 (s, RhO*C*), 97.2 (dd, *C*$_5$Me$_5$), 58.7 (s, CO$_2$*C*H$_2$), 14.7 (s, CH$_3$, Et), and 8.7 (s, C$_5$*Me*$_5$).

$[\mathrm{Rh\{OCC(CO_2Et)SC(CO_2Et)CO\}}(\eta^5\text{-}\mathrm{C_5Me_5})\{\mathrm{P(OPh)_3}\}]\cdot\mathrm{H_2O}$ **2b**·H_2O. A solution of $[\{\mathrm{RhCl_2}(\eta^5\text{-}\mathrm{C_5Me_5})\}_2]$ (77.1 mg, 0.125 mmol), with triphenyl phosphite (77.4 mg, 0.250 mmol) and **Ia** (65 mg, 0.250 mmol) in dichloromethane (20 cm^3) was refluxed with excess silver(I) oxide (*ca.* 0.8 g) for 4 h. The resulting deep yellow-brown solution was filtered to remove the silver salts, and reduced in volume to *ca.* 4 cm^3. Addition of light petroleum (*ca.* 60 cm^3) gave, on standing, brown platy microcrystals of **2b**·H_2O, which were filtered off and dried *in vacuo* (54 mg, 26%) (Found: C, 55.65; H, 5.35. $C_{38}H_{40}O_9PRhS$ requires C, 56.60; H, 5.00. $C_{38}H_{40}O_9PRhS\cdot H_2O$ requires C, 55.35; H, 5.15%), m.p. > 144 °C (decomp.); ν(C=O) at 1662 cm^{-1}. NMR: ^{31}P-{^{1}H}, δ 112.3 [d, ^1J(RhP) 266]; ^{1}H, δ 7.33–7.07 (m, 15 H, Ph), 4.25 [m, second-order, 4 H, CH_2], 2.22 (s, br, 2 H, H_2O), 1.41 [d, 15 H, η^5-C_5Me_5, J(PH) 5.1], and 1.31 [t, 6 H, CH_3 of ethyl, ^3J(HH) 7.1]; ^{13}C-{^{1}H}, δ 172.8 (s, RhOC*C*), 163.8 (s, *C*O$_2$Et), 150.8 [d, C^1, Ph, ^2J(PC) 8.1], 129.8 (s, C^3, Ph), 124.9 (s, C^4, Ph), 120.4 [d, C^2, Ph, ^3J(PC) 5.1], 100.0 (dd, *C*$_5$Me$_5$), 99.7 (s, RhO*C*), 59.0 (s, CO$_2$*C*H$_2$), 14.8 (s, CH$_3$, Et) and 8.6 (s, C$_5$*Me*$_5$).

$[\mathrm{Rh\{OCC(CO_2Et)OC(CO_2Et)CO\}}(\eta^5\text{-}\mathrm{C_5Me_5})(\mathrm{py})]\cdot 2\mathrm{H_2O}$ **2c**·$2H_2O$. A solution of $[\{\mathrm{RhCl_2}(\eta^5\text{-}\mathrm{C_5Me_5})\}_2]$ (120 mg, 0.194 mmol) in dichloromethane (25 cm^3) with pyridine (4 drops, excess) and **Ib** (95 mg, 0.389 mmol) was refluxed with excess silver(I) oxide (*ca.* 0.7 g) for 1 h. The resulting bright orange solution was filtered to remove the silver salts, and evaporated to dryness under reduced pressure. The resulting oily solid was dissolved in dichloromethane (4 cm^3), and slow addition of light petroleum (*ca.* 70 cm^3) gave, on standing, orange microcrystals of **2c**·$2H_2O$ (165 mg, 71%). Slow recrystallisation from dichloromethane–light petroleum gave orange crystals for elemental microanalysis (Found: C, 50.10; H, 5.70; N, 2.30. $C_{25}H_{30}NO_7Rh$ requires C, 53.70; H, 5.70; N, 2.50%. $C_{25}H_{30}NO_7Rh\cdot 2H_2O$ requires C, 50.45; H, 5.75; N, 2.35%), m.p. > 170 °C (decomp.); ν(C=O) at 1698 cm^{-1}. NMR: ^{1}H, δ 8.67–7.28 (m, 5 H, py), 4.16 [q, 4 H, CH_2, ^3J(HH) 7.1], 1.58 [s, 15 H, η^5-C_5Me_5], and 1.23 [t, 6 H, CH_3 of ethyl, ^3J(HH) 7.1 Hz].

Crystal Structure Determination of **2a**·H_2O.—A red crystal of approximate dimensions 0.58 × 0.36 × 0.32 mm was glued to the end of a thin glass fibre using epoxy resin. Crystal data are reported in Table 1. Intensity data were measured on a Siemens P4 diffractometer at 293 K, using Mo-Kα radiation (λ = 0.710 73 Å), and an ω-scans method. 8571 Reflections were measured over the range $2.67 < \theta < 26.00°$ with $-1 \leqslant h \leqslant 16$, $-1 \leqslant k \leqslant 21$ and $-18 \leqslant l \leqslant 18$. The reflections were corrected for Lorentz and polarisation effects and merged to give 7100 independent reflections ($R_{\mathrm{int}} = 0.0271$).

The structure was solved by direct methods using the program SHELXTL-PC[19] and refined using the program SHELXL 93[20] with full-matrix least squares on F^2. The ratio of data : restraints : parameters was 7100 : 0 : 433. The orientation of the methyl hydrogens was established from difference Fourier maps. The methyl hydrogen atom positions were then idealised, and treated as all other hydrogen atoms, with the H atoms riding on the carbon atoms (C–H 0.96 Å), and a common fixed isotropic displacement parameter (0.08 Å^2). All other atoms were refined with anisotropic thermal parameters. Final cycles of refinement gave $R1 = 0.0407$, $wR2 = 0.0957$ for all data, $R1 = \Sigma||F_o| - |F_c||/\Sigma|F_o|$, $wR2 = [\Sigma w(F_o^2 - F_c^2)^2/\Sigma w(F_o^2)^2]^{\frac{1}{2}}$, $w = 1/[\sigma^2(F_o^2) + (0.0377P)^2 + 1.90P]$ and $P = [max(F_o^2, 0) + 2F_c^2]/3$. The maximum and minimum electron densities in the final ΔF map were 0.330 and -0.363 e Å^{-3} respectively.

Additional material available from the Cambridge Crystallographic Data Centre comprises H-atom coordinates, thermal parameters and remaining bond lengths and angles.

Acknowledgements

We thank the Universities of Waikato and Leicester for financial support, and the New Zealand Lottery Grants Board for a grant-in-aid towards the purchase of a mass spectrometer. W. H. thanks Mrs. A. Upreti for IR spectra.

References

1 C. G. Pierpont and R. M. Buchanan, *Coord. Chem. Rev.*, 1981, **38**, 45; *Comprehensive Coordination Chemistry*, ed. G. Wilkinson, Pergamon, Oxford, 1987, vol. 5.

2 For recent examples see: O.-S. Jung and C. G. Pierpont, *Inorg. Chem.*, 1994, **33**, 2227; O.-S. Jung and C. G. Pierpont, *J. Am. Chem. Soc.*, 1994, **116**, 2229; D. M. Adams, A. Dei, A. L. Rheingold and D. N. Hendrickson, *J. Am. Chem. Soc.*, 1993, **115**, 8221; O. Carugo, C. B. Castellani, K. Djinovi'c, and M. Rizzi, *J. Chem. Soc., Dalton Trans.*, 1992, 837; G. A. Fox and C. G. Pierpont, *Inorg. Chem.*, 1992, **31**, 3718.

3 O. Gandolfi, G. Dolcetti, M. Ghedini and M. Cais, *Inorg. Chem.*, 1980, **19**, 1785.

4 C. A. McAuliffe, H. L. Sharma and N. D. Tinker, in *Studies in Inorganic Chemistry 11. Chemistry of the Platinum Group Metals. Recent Developments*, Elsevier, Amsterdam, 1991, pp. 571–572.

5 J. Suh, S. H. Lee and H. Paik, *Inorg. Chem.*, 1994, **33**, 3; T. D. P. Stack, T. B. Karpishin and K. N. Raymond, *J. Am. Chem. Soc.*, 1992, **114**, 1512; T. B. Karpishin and K. N. Raymond, *Angew. Chem., Int. Ed. Engl.*, 1992, **31**, 466.

6 S. Kawata, S. Kitagawa, M. Kondo, I. Furuchi and M. Munakata, *Angew. Chem., Int. Ed. Engl.*, 1994, **33**, 1759; S. G. Jonasdottir, C. G. Kim and D. Coucouvanis, *Inorg. Chem.*, 1993, **32**, 3591; G. A. Fox, S. Bhattacharya and C. G. Pierpont, *Inorg. Chem.*, 1991, **30**, 2895.

7 J. A. Daldy, J. Fawcett, W. Henderson, R. D. W. Kemmitt and D. R. Russell, *J. Chem. Soc., Dalton Trans.*, 1994, 3383.

8 J. W. Kang, K. Moseley and P. M. Maitlis, *J. Am. Chem. Soc.*, 1969, **91**, 5970.

9 K. Isobe, P. M. Bailey and P. M. Maitlis, *J. Chem. Soc., Dalton Trans.*, 1981, 2003.

10 P. Espinet, P. M. Bailey and P. M. Maitlis, *J. Chem. Soc., Dalton Trans.*, 1979, 1542.

11 A. L. Balch, V. J. Catalano and M. M. Olmstead, *Inorg. Chem.*, 1990, **29**, 1638; J. A. Ladd, M. M. Olmstead and A. L. Balch, *Inorg. Chem.*, 1984, **23**, 2318.

12 L. Manojlovic-Muir and K. W. Muir, *Acta Crystallogr., Sect. A*, 1975, **31**, S132; C. W. Lange, M. Foldeaki, V. I. Nevodchikov, V. K. Cherkasov, G. A. Abakumov and C. G. Pierpont, *J. Am. Chem. Soc.*, 1992, **114**, 4220; M. A. Calvo, A. M. M. Lanfredi, L. A. Oro, M. R. Pinillos, C. Tejel, A. Tiripicchio and F. Ugozzoli, *Inorg. Chem.*, 1993, **32**, 1147; J. G. Leipoldt, L. D. C. Bok, S. S. Basson and H. Meyer, *Inorg. Chim. Acta*, 1980, **42**, 105; L. N. Zakarov, Y. T. Struchkov, G. A. Abakumov and V. I. Nevodchikov, *Koord. Khim.*, 1990, **16**, 1101.

13 M. B. Hursthouse, K. M. A. Malik, D. M. P. Mingos and S. D. Willoughby, *J. Organomet. Chem.*, 1980, **192**, 235.

14 R. D. Voyksner, *Environ. Sci. Technol.*, 1994, **28**, 118A.

15 For some recent examples, see: X. Xu, S. P. Nolan and R. B. Cole, *Anal. Chem.*, 1994, **66**, 119; D. Dakternieks, H. Zhu, E. R. T. Tiekink and R. Colton, *J. Organomet. Chem.*, 1994, **476**, 33; T. J. Cardwell, R. Colton, S. Mitchell and J. C. Traeger, *Inorg. Chim. Acta*, 1994, **216**, 75; A. van den Bergen, R. Colton, M. Percy and B. O. West, *Inorg. Chem.*, 1993, **32**, 3408.

16 See, for example, A. M. Bond, R. Colton, A. D'Agostino, J. Harvey and J. C. Traeger, *Inorg. Chem*, 1993, **32**, 3952.

17 C. W. Bird and G. W. H. Cheeseman, in *Comprehensive Heterocyclic Chemistry*, eds. C. W. Bird and G. W. H. Cheeseman, Pergamon, Oxford, 1984, vol. 4.

18 W. Henderson, unpublished work.

19 G. M. Sheldrick, SHELXTL PC, Release 4.2, Siemens Analytical X-Ray Instruments, Madison, WI, 1991.

20 G. M. Sheldrick, SHELXL 93, Program for Crystal Structure Refinement, University of Göttingen, 1993.

Received 31*st January* 1995; *Paper* 5/00575B